

Negative differential resistance of Styrene on an ideal Si[111] surface: dependence of the I-V characteristics on geometry, surface doping and shape of the STM-tip

Samuel E. Baltazar,^{1,2,*} Mario De Menech,^{2,3} Ulf Saalmann,³ Aldo H. Romero,⁴ and Martin E. Garcia²

¹*Advanced Materials Department, IPICYT, Camino Presa San José 2055, 78216, San Luis Potosí, S.L.P., México*

²*Theoretische Physik, Fachbereich Naturwissenschaften, and Center for Interdisciplinary Nanostructure Science and Technology (CINSaT), Universität Kassel, Heinrich-Plett-Str. 40, 34132 Kassel, Germany.*

³*Max-Planck-Institut für Physik komplexer Systeme Nöthnitzer Str. 38, 01187 Dresden, Germany*

⁴*CINVESTAV Querétaro, Libramiento Norponiente No 2000, 76230 Querétaro, México*

(Dated: October 30, 2021)

Abstract

We study the electron transport properties through a supported organic molecule styrene (C_8H_8) on an ideal silicon surface Si[111] and probed by a STM-tip. The I-V characteristics and the differential conductance of the molecule are calculated using a self consistent approach based on non equilibrium Green's functions. Two different adsorption configurations for the molecule on the surface were considered which corresponds to a global and a local minimum of the total energy. In both cases we find a negative differential resistance (NDR) in a given interval of bias voltages. This effect is controlled by the states available close to the Fermi level of the surface and can be manipulated by properly doping the substrate. We also analyze the influence of the tip-shape on the I-V characteristics.

I. INTRODUCTION

Transport properties through supported molecules on substrates are an interesting phenomena in the field of nanodispositives. This idea has been extensively studied in the last few years mainly due to the possibility to build electronic dispositives at atomic scale. The major bottle neck in nanoelectronics is to have different mechanisms to control the transport properties as wish. In order to get to this point experiments and theory should work together by investigating different molecules, substrates and physical properties to achieve this goal. In the case of substrates, two different approaches have been followed by using metallic or semiconductor surfaces as the electrodes which interact with a given molecule. With metallic contacts, the conduction could be described through an ohmic behavior, but if non-metallic contacts are considered (where the surface can have gaps in the electronic dispersion relation or if the molecule and surface interaction is able to open a gap), the electronic transport could change. Changing the molecule type has been also further investigated and many interesting results could be found in the literature. Some examples about electronic transport in mesoscopic systems consider carbon nanotubes used as nanowires ¹, metal-ion clusters useful for information storage ² and molecules such as small silicon clusters that have been then studied showing resonant tunneling effects due to the electronic states of the cluster³. In the particular the case of silicon clusters in contact with semiconductor surface have been theoretically investigated in our group. We did report a diode-like behavior, opening the possibility of using a like dispositive in the the design of new electronic dispositives⁴. Channels responsible of the electronic flow are not only established by the molecular levels of the molecule, but also by the position of the Fermi level associated with the surface. Recently, negative differential resistance (NDR) on heavily doped Si substrates in contact with organic molecules has been predicted theoretically⁵ and demonstrated experimentally⁶. This observation has been related to the crossing of the HOMO or LUMO levels of the band edge of the underlying semiconductor. It has been also pointed out that by using different molecules such as metallic nanocrystals or organic molecules, the conductance can be changed to be diode-like behavior and showing a dependence on the used molecules ^{7,8}. These recent results have reinforced the idea of using molecular systems as active structures in electronic components at nano scale.

In this work, we want to consider the electronic transport through an organic molecule in

contact with a semiconductor surface. We report and explain a non-ohmic behavior in the electronic transport and we relate this observation to the interaction between the different systems. Transport properties are also tested under different conditions, such as doping and applied external electric fields.

II. FORMALISM

In this section we draw the methodology we have followed to calculate the transport properties here reported. This methodology has been previously presented by De Menech to study silver clusters and C₆₀ fullerenes on metal surfaces *et al.*^{9,10}. Our system consists of substrate-molecule-electrode. The surface has been modeled as an ideal structure with no reconstruction after the molecule has been absorbed on it. The electrode is a metallic tip far away from the molecule, with no bonding with it. The transport properties at equilibrium and non-equilibrium conditions were calculated using a Green's functions approach. The electronic states are described by means of a semiempirical extended Hückel theory (EHT), where parameters are obtained from first principle calculations¹¹. We did guarantee a very good agreement between our electronic description and *ab initio* calculations, with errors less than 2% around the Fermi energy.

From the Hamiltonian of a molecule H_{mol} and a contact H_C , a coupled system (contact C - molecule) can be described by the composite Schrodinger equation

$$[(E + i\eta)S - H]G(E) = 1, \quad \eta \rightarrow 0^+ \quad (1)$$

where S is the normalization matrix and G is the Green's function of the total system. By using the Green's function, the spectral function (density of states per unit energy) can be written as

$$A(E) = -\frac{2}{\pi} \text{Im}[G(E)] \quad (2)$$

for the spin unpolarized case. Following this description, the local density of states can be written as

$$\rho(r, E) = \sum_{\mu\nu} A_{\mu\nu}(E) \psi_\mu \psi_\nu \quad (3)$$

where ψ s are the molecular wavefunctions, giving rise to the electronic density as

$$n(r) = \int_{-\infty}^{E_F} dE \rho(r, E) \quad (4)$$

that considers the integration just until the Fermi energy level.

Now, if we want to study the consequences on a specific part of the system due to the presence of the other parts, the Green's function approach allows it by including the effect as perturbations on the original Green function. This approach has been described by Williams *et al.*¹² to study defects in crystals as perturbations. They have showed that the problem can be described by a Dyson equation and have obtained the Green's function of the perturbed system. In our case, the Dyson equation leads to the perturbed Green's function of the cluster due to the presence of the surface. The surface effects are included as

$$G(E) = G^0(E) + G^0(E)\Sigma G(E) \quad (5)$$

where G^0 and G are the Green's functions associated with the isolated (unperturbed part) and the supported cluster (perturbed) respectively, and Σ is the self-energy matrix given by:

$$\Sigma = \tau G_s^0(E) \tau^\dagger. \quad (6)$$

The previous equation takes into account the effect of the surface, which could come as broadening and shifting of molecular energy levels (the size of G , G^0 and Σ are defined mainly from the molecular orbitals values). The term $G_s^0(E)$ corresponds to the Green's function of the isolated surface and τ is the coupling matrix between the cluster and the surface. The non equilibrium regime, is considered when another electrode is added to the system and an external voltage is applied between the surface and the electrode. In this case, the representation for the supported cluster is changed by using the correlation function $G^< = G\Sigma^<G^<$ to determine the charge density at a specific bias V . The term $\Sigma^< = i(f(E - \mu_s)\Gamma^s + f(E - \mu_e)\Gamma^e)$ is the lesser self-energy that depends on the Fermi function $f_i = f(E - \mu_i)$ of the contact i (surface and electrode) for a specific chemical potential μ and the broadening matrix Γ of the surface and the metallic electrode. The rate at which electrons goes from one contact to another through the cluster is the transmittance $T(E, V)$. By considering only coherent transport (no scattering), it is possible to show that $T(E, V)$ can be evaluated using the relation

$$T \equiv Tr[\Gamma^s G \Gamma^e G^\dagger]. \quad (7)$$

Finally, the expression used to calculate the current through a system like the one depicted in fig. 1, where a molecule, with discrete energy levels, is located between a semiconductor

surface and an electrode (with a uniform distribution of states), can be written as

$$I = \frac{2e}{h} \int_{-\infty}^{\infty} dET(E)[f_1 - f_2]. \quad (8)$$

The transmittance $T(E)$ is integrated in the energy interval associated with each applied bias voltage and restricted by the Fermi function of the contacts. For both cases (surface and electrode), local equilibrium is assumed and, in principle, the low temperatures approximation is used, so the integration can be performed between μ_1 and μ_2 .

After the calculation of the transmittance is performed, we did follow the treatment given

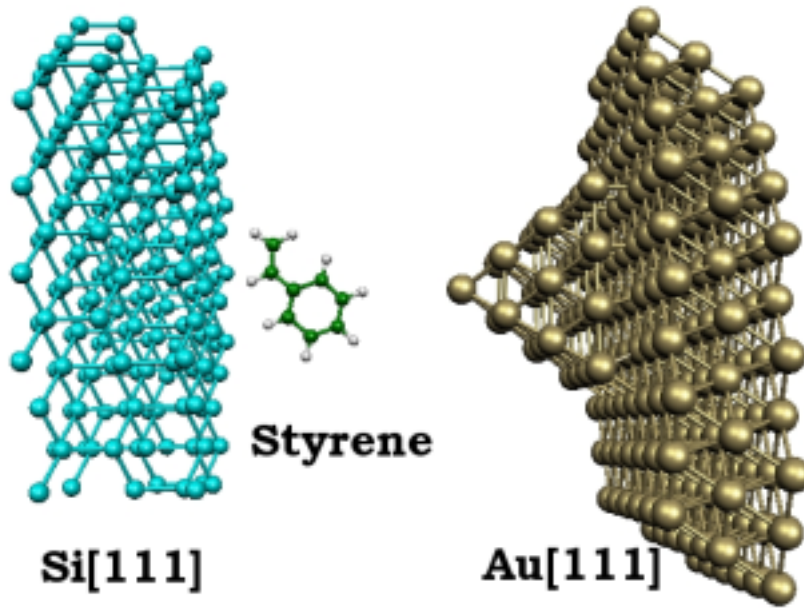


FIG. 1: Atomic configuration of an organic molecule interacting, at a given optimal distance, with a semiconducting surface Si[111] and a metallic electrode Au[111] used as a STM probe.

by Tian *et al.*¹³ to obtain the conductance and the differential conductance. At low temperature regime, the conductance will be proportional to the transmittance (at zero bias), where the differential conductance will be written as

$$\frac{dI}{dV} \approx G_0 T(E_f + eV) \quad (9)$$

where $G_0 = 2e^2/h$ is the maximum conductance constant. Here it is assumed that the electrostatic potential modifies mostly the chemical potential of the metallic electrode. To describe the molecular electronic properties we use the EHT approach, where the electronic

Hamiltonian is parameterized through the matrix elements $H_{\alpha i, \beta j}$, between two atomic orbitals α and β of atoms i and j respectively and assumed to be proportional to the overlap $O_{\alpha i, \beta j}$ and such that $H_{\alpha i, \beta j} = K_{\alpha i, \beta j} \cdot O_{\alpha i, \beta j}$. According with Cerda *et al.*¹¹, the parameter $K_{\alpha i, \beta j}$ can be defined from the on site energies using the form: $K_{\alpha i, \beta j} = K_{EHT} \cdot (E_{\alpha i} + E_{\beta j})/2$, where K_{EHT} is a fitting parameter usually obtained for solids and calculated from first principles. In our case this value was fixed at 1.75 for H, 2.8 for C and 2.3 for Au and Si.

In order to evaluate the accuracy of this model, we have compared the description obtained with the EHT model, with a calculation based on a plane wave implementation of the density functional theory with normalized pseudo potentials, as implemented in CPMD¹⁴. The exchange-correlation has been described by using the local spin density approximation (LSDA)^{15,16}. The atomic structure and energy minimization of the isolated molecule and the supported molecule in contact with the surface have been calculated at the same theory level.

III. RESULTS

In order to make a proper electronic characterization of the system, we did start by describing every one of the system components as isolated systems. The surface considered in this work is a semiconductor silicon with a [111] orientation and no reconstruction. Even though, it is experimentally more typical to find this surface as reconstructed in (2x1) and (7x7), depending on temperature^{3,17}, it has been also possible to obtain a Si[111]- in a (1x1) surface reconstruction¹⁸. For the unreconstructed surface, the dangling bonds are associated to the discrete energy levels that can be observed at the band structure of the Si[111] surface. In the case of the molecule, we have selected styrene (C_8H_8) as the organic molecule in contact with the surface. This molecule has been previously considered and experimentally studied as a possible component in the design of new molecular devices⁶. For the coupled case, the interaction between the organic molecule and the Si[111] surface has been obtained from a geometrical optimization from first principle calculations. The final atomic structure feed to the transport calculation is the lowest energy geometry. The structural optimization has been obtained considering the local spin density approximation (LSDA) as the exchange and correlation terms¹⁹. From the optimization, we have obtained two possible structural configurations for the supported molecule, labeled as case A and B

from now and on. The optimization also defines the optimal distance between the molecule and the surface. The energy difference between both configurations is 15.8 eV, being case B the most stable. This result was calculated using a computational package Gaussian 98²⁰

A. C_8H_8 on Si[111] : (case A)

For the case named as A, the energy difference between the HOMO and LUMO levels of the free molecule is 0.95 eV. Whereas, in the coupled case, the electronic gap is obviously reduced and the optimal molecule-surface distance is found to be 2.5 ang. By using the minimal structure, the electronic structure is calculated using the EHT model (as previously discussed). A fair comparison with the electronic levels from ab-initio calculations was found. In order to evaluate equilibrium properties we have considered

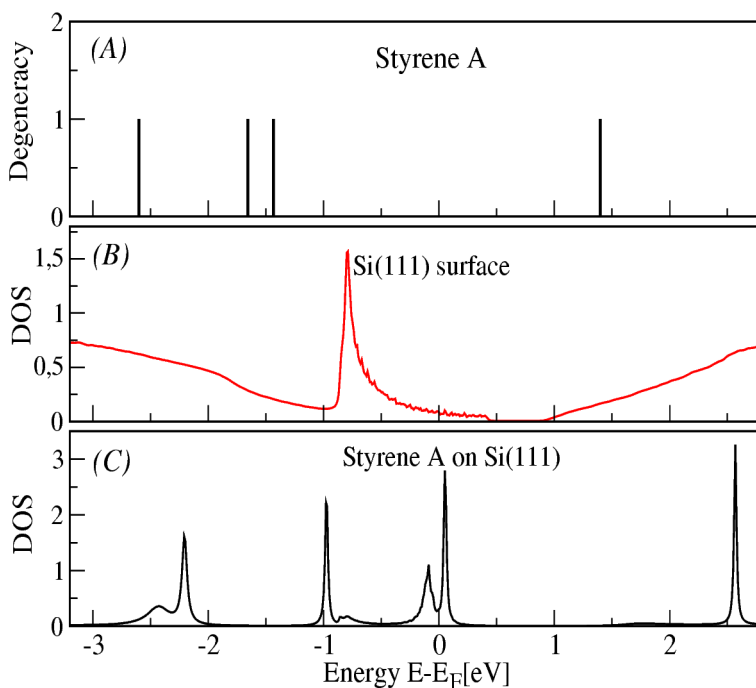


FIG. 2: Electronic structure of the C_8H_8 -Si[111] system. Graph A shows the energy levels of C_8H_8 (A case) for the isolated case, whereas B shows the DOS of Si[111] and finally C corresponds to the DOS of C_8H_8 on ideal Si[111]. Energy values are shifted respect to the Fermi level.

Figure 2 that shows the electronic density of states of the system calculated within the EHT approach. In Fig. 2-A the electronic levels of the free molecule are presented. In Fig. 2-B, the e-DOS of the Si[111] surface is shown. An electronic gap of 0.45 is observed

and dangling bonds are located around 0.7 eV below the Fermi level. This description is in good agreement with results reported by Pandey²¹ and Schlüter²², obtained using a semiempirical tight-binding method and a self-consistent pseudopotential respectively. The presence of the dangling bonds is observed in these cases with a shift of the states compared with our results and given because of the parameterization of the considered model. Finally, in Fig. 2-C the e-DOS of the molecule interacting with the surface is shown. The energy levels of the free cluster are broadened and red shifted (moved to the right side) in the coupled case. As a consequence, there are more states close to the Fermi level and the gap of the surface.

Once we have established the equilibrium conditions, a metallic electrode is included in the system to evaluate transport properties. As a first approach, an ideal Au(111) surface is considered as an electrode. Initially, the electrode and surface are initially at local equilibrium and with chemical potentials $\mu_e = -5.26$ eV and $\mu_s = -4.8$ eV respectively²³. Under non-equilibrium conditions, an external bias V is imposed by changing the chemical

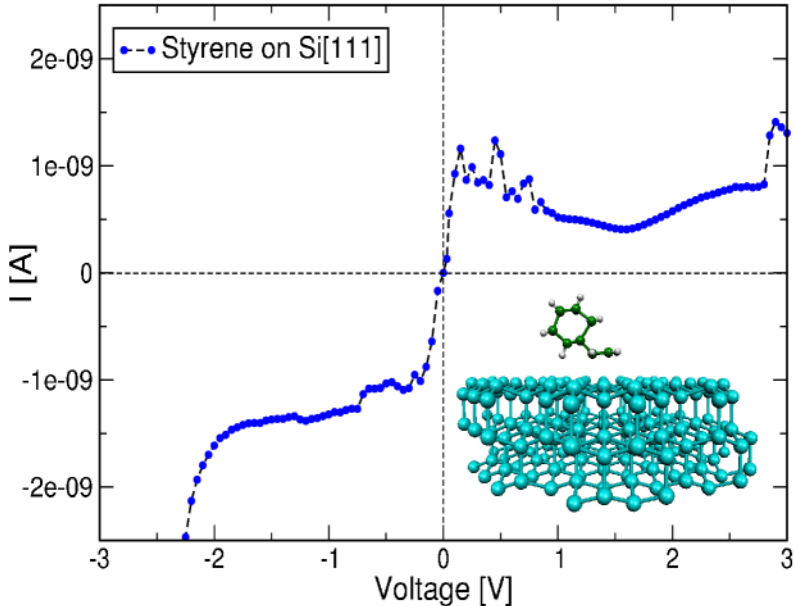


FIG. 3: I-V characteristics of the system as a function of voltage and considering an interval of -3.0 and 3.0 V.

potential of the metallic electrode. Then the transmittance $T(E,V)$ is calculated and the current can be obtained integrating the transmittance in the energy range associated to each bias. I-V curve is shown in Fig. 3 where the applied bias goes from -3 to 3 V.

We can observe a NDR effect for a positive applied bias. The intensity of the current starts to decrease at 0.7 V finding a minimum around 1.5 V where the current starts to increase again. This effect has been also experimentally reported for styrene on Si[100] ⁶. In this case, we have evaluated the states close to the Fermi level finding a shifting effect (adjustment of the position of molecular levels) as a function of the applied bias in the DOS and a drop in the transmittance when the bias is larger than 0.5 V. The molecular state, located next to the Fermi level (see Fig. 2-C), will be crucial when we have to explain the major contribution to the NDR effect. This state is the main peak in the DOS located in the right side of the DOS respect to the Fermi level (that in this case was considered at -4.8 eV for Si[111]) and the charge distribution associated to it is located mainly between the molecule and the silicon surface. In Fig. 4 the DOS of the styrene molecule is compared with the differential conductance dI/dV as a function of bias. In the case of dI/dV , we can

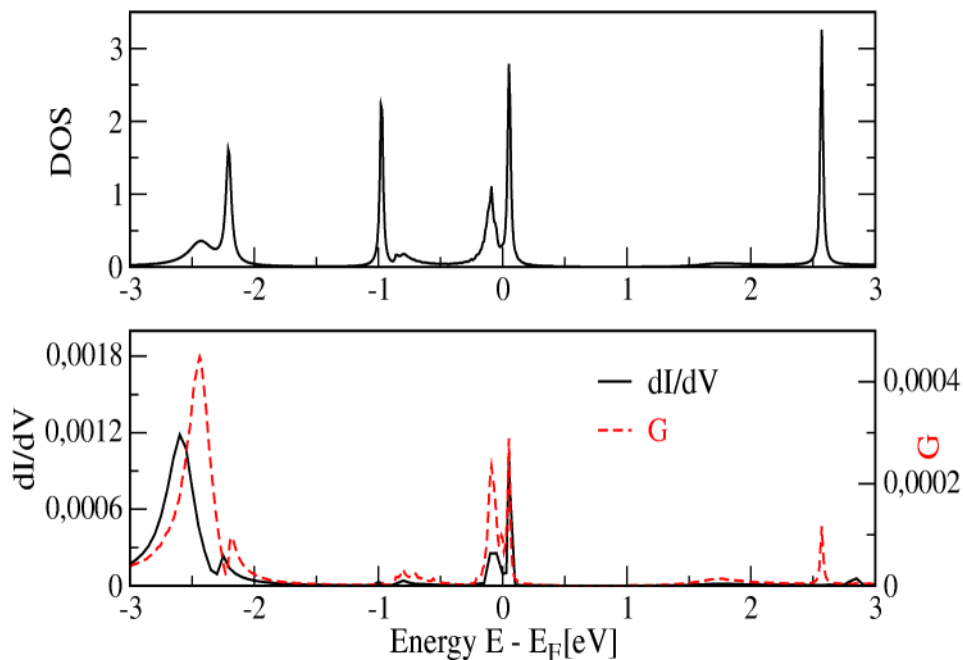


FIG. 4: Calculated DOS and differential conductance dI/dV .

see not just the shift of the peaks respect to the e-DOS but also the magnitude of some peaks clearly changing, when they are compared to other peaks also observed in the e-DOS. The dI/dV characteristic in Figure 4 shows the molecular states that indeed contribute to the electronic transport in the system. In this context, the intensity of the two peaks located at ± 0.2 eV respect to the Fermi level are clearly defined, in contrast to the

state located 1 eV below the Fermi level. Another parameter we did take into account is related to the doping on the surface. To consider doped surfaces, a simple approximation can be performed without the inclusion of atoms in the system, such as P or S. This can be achieved by modifying the Fermi level of the substrate. We have considered three cases where the chemical potential of the surface is assumed to be $\mu_s = -4.8$ eV (initial case), -4.3 eV (n-type) and -5.3 eV (p-type). For each case, there are different equilibrium conditions controlled by the chemical potential. We have calculated the transmittance in the system and then the current $I(V)$. These results have been depicted in Fig. 5 where a voltage range from -3 to 3 V has been used. In this figure we can see that the n-type surface shows a similar behavior compared to the non-doped case ($\mu_s = -4.8$ eV), where the NDR effect at positive bias is observed. In the case of the p-type surface the result is rather different. The NDR is not found at positive bias and even the behavior at negative V is also different when it is compared with the previous cases. In order to understand the differences at each

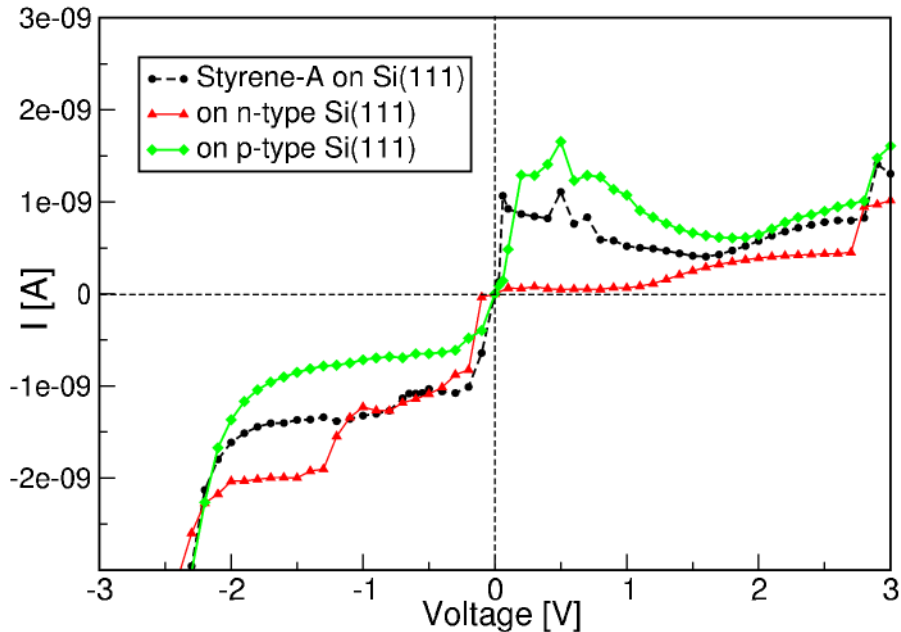


FIG. 5: I-V characteristics for doped surfaces. To consider doped surfaces, the surface chemical potential μ_s is adjusted considering three cases: $\mu_s = -4.8$ eV (initial case), -4.3 eV (n-type) and -5.3 eV (p-type).

doped or undoped surface Fig. 6 shows the e-DOS and the differential conductance dI/dV . Even considering that the peaks of e-DOS are clearly shown at each case, we can see a displacement of the peaks as well as a change in their magnitude. In the case of dI/dV ,

the peaks are again shifted and changed in magnitude. One of the important aspect of the doping effect, is that molecular states have been also shifted according to each doped case and, in particular, the n-type surface ($\mu_s = -4.3eV$) have moved (red shifted) the molecular states to the region of the calculated energy gap for the Si[111] surface (see Fig. 2). In order to differentiate the influence of the tip geometry, we did consider two

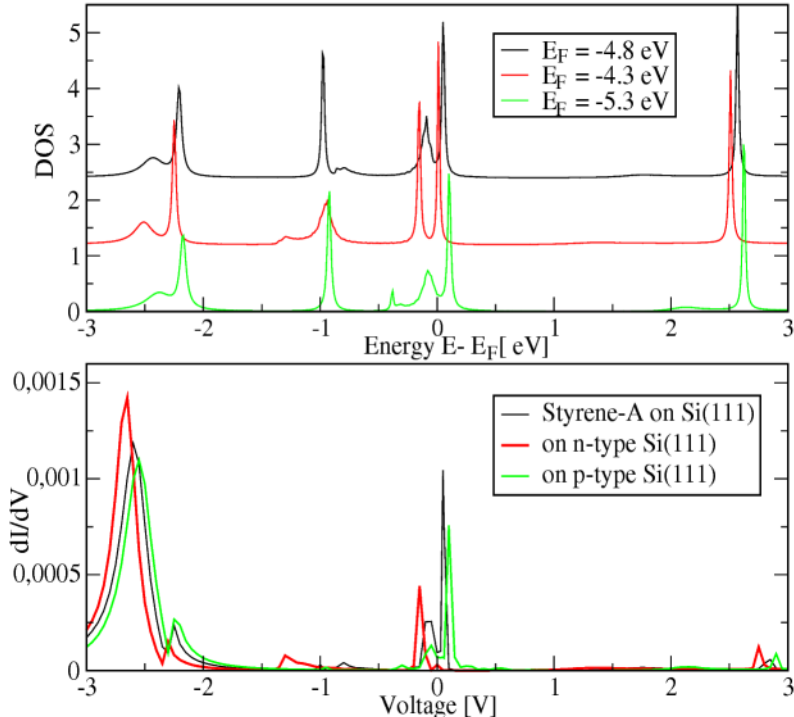


FIG. 6: DOS and dI/dV characteristics for doped surfaces. To consider doped surfaces, the surface chemical potential μ_s is adjusted to consider initial case, a p-type and a n-type surface.

different geometries: a flat surface and a pyramidal structure. The last geometry is shown in Fig. 7 where the tip shape is obtained with 30 Au atoms. The molecule-tip distance has been fixed to 5.0 ang. For the flat electrode, we have considered a distance of 5.2 ang. These distances are long enough to consider only tunneling current between the molecule and the tip/electrode. Fig. 7 shows the I-V characteristics with and without a tip. In the case of the tip, the intensity of the current was multiplied by 5 for better comparison. We can see that at low voltages (positive and negative), the behavior is rather similar between them, but this description changes when the bias is higher in the positive direction. The NDR effect observed in the case of the flat electrode, has been diminished until disappear, showing in contrast an almost constant behavior when a bias between 0.5 and 1.5 V is

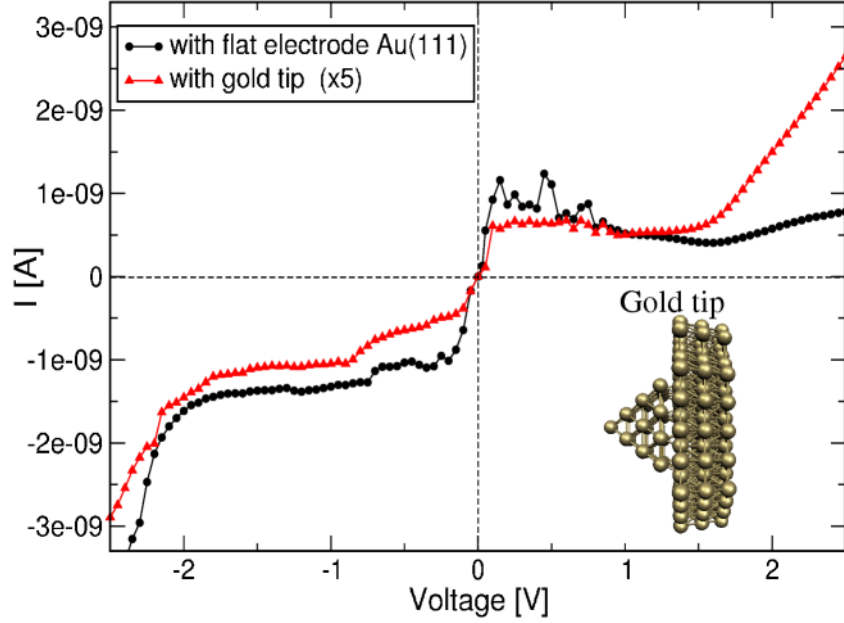


FIG. 7: I-V characteristics considering different probes. Results using a flat electrode are compared two gold tips.

applied. The calculated e-DOS and the dI/dV in Fig. 8 show the comparison between the

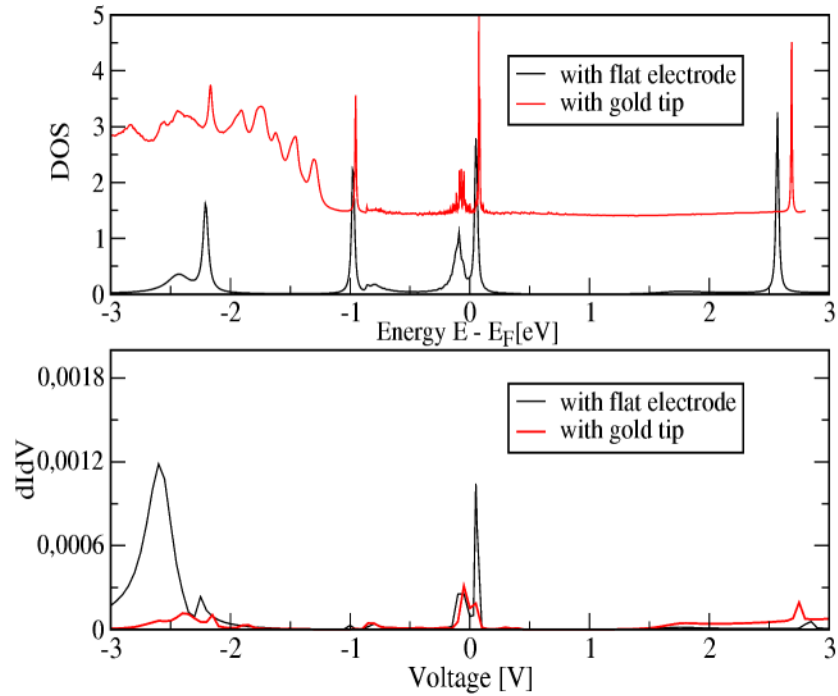


FIG. 8: DOS and dI/dV characteristics considering different probes. Results using a flat electrode are compared two gold tips.

flat electrode and the tip, in particular, a change in the magnitude of the peak located at 0.2 eV above the Fermi level, where the intensity is diminished when the tip is considered. There is also another difference mainly localized at lower energies and can be attributed to the considered tip.

B. C_8H_8 on Si[111]: B case

The previous discussed molecular geometry is the one which has attracted more attention when it is supported by Si[100] surface⁶. Nevertheless, We have found a second, stable configuration (B case) when the styrene molecule is interacting with the Si[111] with no reconstruction. Is important to notice that the energetic optimization shows that $E(\text{case B}) < E(\text{case A})$, which means that this configuration is much more stable. In this case, the optimal distance between the molecule (H atoms) and the surface (Si atoms) was found at 2.8 ang. Figure 9 shows that energy levels associated with the case B free molecule

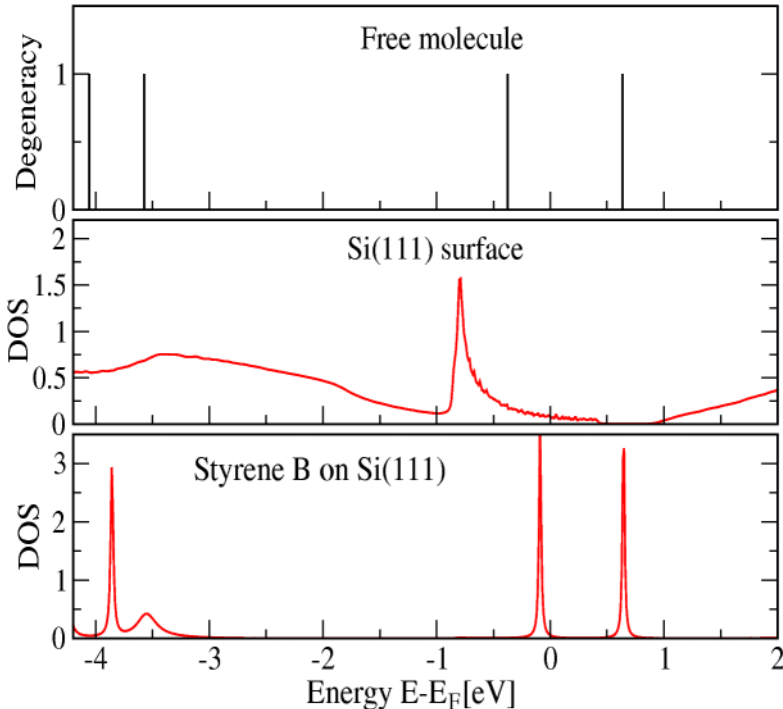


FIG. 9: Electronic structure of the C_8H_8 (B case) -Si[111] system. Graph A shows the energy levels of C_8H_8 for the isolated case, whereas B shows the DOS of Si[111] and finally C corresponds to the DOS of C_8H_8 on ideal Si[111].

(graph A) and the e-DOS of the Si[111] surface (graph B) and the molecular levels for the molecule interacting with the surface (graph C). From the e-DOS of the supported molecule, we can see molecular levels energetically located not only close, but also in the energy gap associated to the surface (graph B in Fig. 9). The two molecular states localized around 0 and 0.7 correspond to the original LUMO and LUMO+1 states respectively and they play an important role in the conduction phenomena. After we have evaluated the electronic configuration at equilibrium conditions (without bias), the I-V curve is shown in Fig. 10 with the same voltage range as case A. Interestingly, the I-V characteristic does not seem to show a similar NDR effect when a positive bias is applied, like in the first case. Instead of this effect, there is no an important contribution for the current at low positive voltages until a bias of 2.0 V is applied. Instead, when the negative bias is considered, there is current flow even at low voltages. If we want to know about the states that participate in

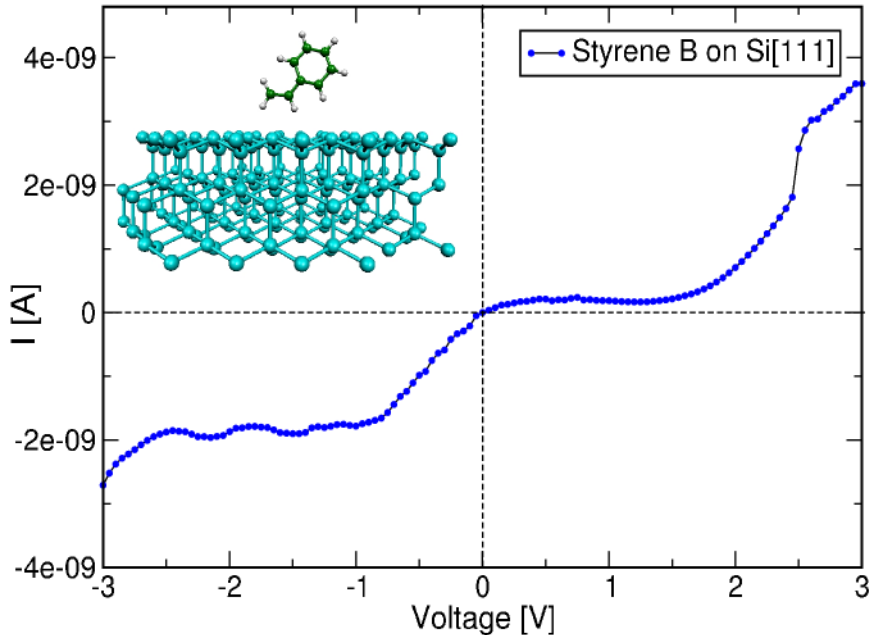


FIG. 10: I-V characteristics of the system as a function of voltage.

the electronic transport, it is possible to evaluate the differential conductance dI/dV and the conductance G in Fig. 11. In this case, the contribution of the state located initially at 0.7 eV above the Fermi level, has a very small intensity in dI/dV characteristic compared to other states. Even the conductance and the dI/dV of the state located at 0.2 eV below the Fermi level, is also small in comparison to, for example, the states located at 2.3 eV above the Fermi level. There is also a spread distribution of the conductance and dI/dV

characteristics for low negative values (between -1.0 and 0.2 eV below E_F). In this case, there will be important to notice that this distribution is located in the same energy interval associated to the dangling bonds on the silicon surface. Following the same lines than in

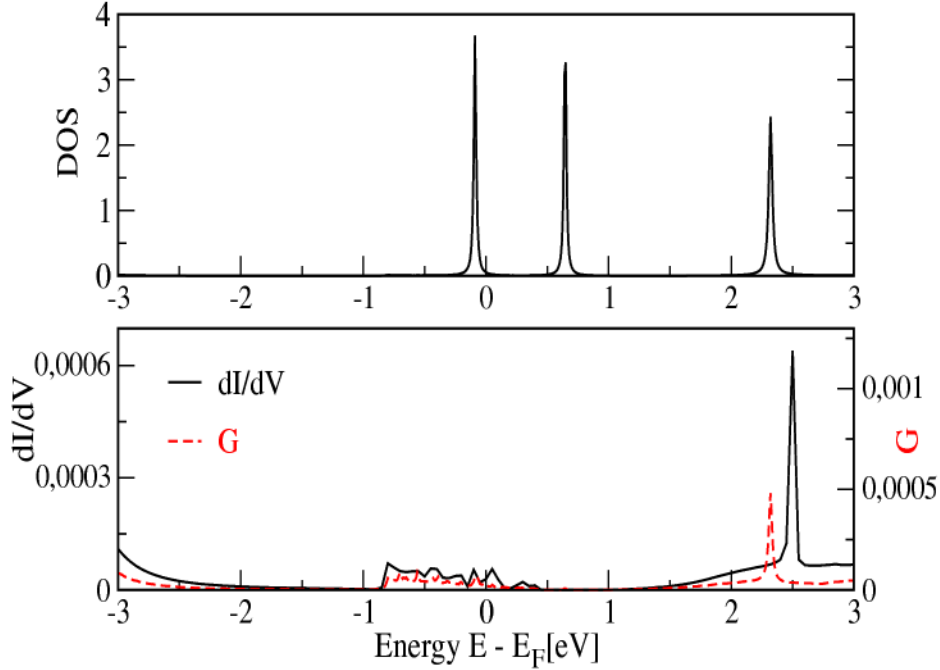


FIG. 11: DOS and dI/dV characteristics of the system as a function of voltage.

the previous configuration, we did also study the transport properties as function of surface doping. As previously explained, we did obtain these conditions by modifying the chemical potential. Results for the I-V characteristics are shown in Fig. 12. This figure shows clearly different results when the substrate is n-type or p-type doped. In the first case, we have the results obtained for C_8H_8 (B case) on Si[111] with a chemical potential of -4.8 eV (original conditions). The current increases steadily after an applied bias of 2.0 V. When the surface is n-type doped (considering $\mu_s = -4.3eV$), there is no response in the current until 0.6 V, where the intensity starts to increase rapidly with the positive applied bias. A completely different behavior is obtained when the surface is p-type (which means that $\mu_s = -5.3eV$). Here we can see that a NDR effect is obtained for the current around 1-2 V, when even if the positive bias is increasing, the current flow is decreasing in magnitude until a minimum value around 2 V. After this bias, the current increases its value again in a similar way like in the two other doped surfaces. The figure 13 shows the DOS and the dI/dV characteristic associated with doped o undoped surface. Here, we notice that the

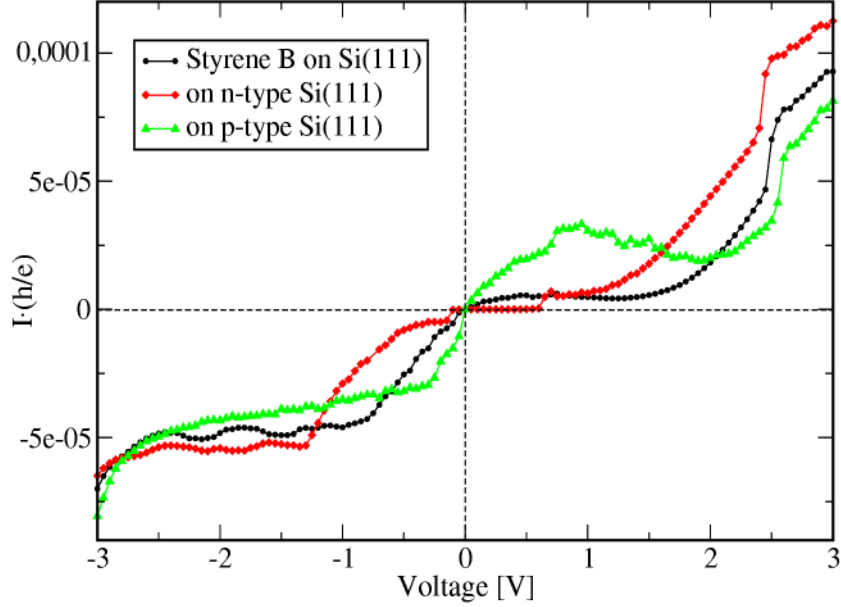


FIG. 12: I-V characteristics for undoped (circles) and doped (diamonds and triangles) surfaces. To consider doped surfaces, the surface chemical potential μ_s is adjusted to each case.

energy has been adjusted to each different Fermi level, so the zero energy position is indeed different for each condition. It is important to notice that even with a similar distribution of the molecular states, the differential conductance looks rather different. For the undoped surface, there is no an important peak for dI/dV at low voltages and the main one is located at 2.4 V, with a spread contribution of states obtained around 0 V. If we consider the n-type Si[111] surface, we can detect an important peak located around 0 V within with the same spread distribution as for the undoped case. For the p-type surface, we can see a small peak around 0.0 V and 2 important peaks, one located around 0.7 V and the other one at 2.5 V. For all doped-undoped surfaces, the same peak, locate around 2.5, is clearly depicted and is related to the state found at 2.4 eV above the Fermi level. Again, the states related to the peaks close to the Fermi level, provide the most important contribution when a low voltage regime is considered.

IV. DISCUSSION AND CONCLUSIONS

Here, we have reported a set of electronic transport calculations for a semiconductor-cluster-electrode system. Initially we have obtained two possible configurations (A and B

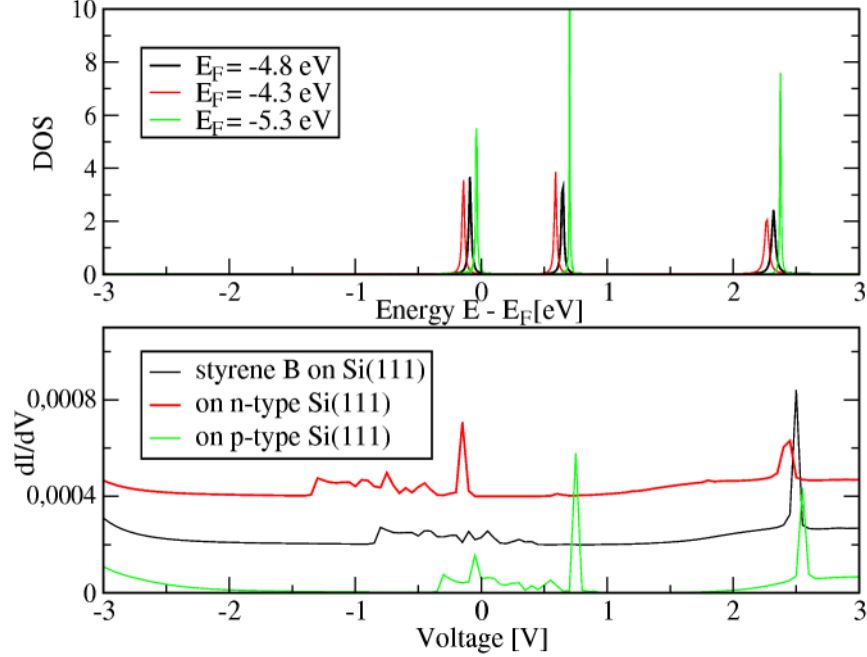


FIG. 13: DOS and dI/dV characteristics for doped surfaces. To consider doped surfaces, the surface chemical potential μ_s is adjusted considering three cases. In the case of dI/dV , values were shifted in intensity for a better description

cases) for the styrene molecule given by the minimization of the energy associated to the surface-molecule system. The most stable configuration corresponds to the B case and the A case corresponds to the atomic configuration of the molecule used for Si[111] surface, as it is shown in Fig. 3. For the A case, we have obtained a NDR effect when a positive bias is applied. This can be understood based on the shifting of the molecular levels, close to the Fermi level, when the voltage is applied. This effect is modulated when the surface has been doped, which changes the chemical potential. This effect is more important for the case of a p-type surface, as it is observed in Fig. 3, when compared to the n-type surface, where the effect is eliminated from the I-V characteristic. This difference is achieved because of the shift of the molecular levels according to each doped surface. For the n-type surface (with $\mu_s = -4.8$ eV), the electronic molecular levels are energetically located inside the energy gap of the silicon surface, so there is no channel available for the electronic transport at low positive bias (see dI/dV curve for n-type surface in Fig. 6). Another result, shows the influence of the tip in the electronic transport, where if the tip is changed, the NDR effect could be diminished with respect to the flat electrode. In order to compare both conditions,

we have used a similar molecule-tip/electrode distance (5 ang.). This can be understood from the potential created by the tip-surface, which is smaller than the potential created by the electrode-surface case. A smaller electric field created for a sharp tip promotes a very small shift of the energy levels of the molecule and then it is more difficult to move the states to the energy interval associated to the energy gap of Si[111]. For the second configuration (B case), the situation is rather different because there is no NDR when the undoped surface is considered. This can be concluded by observing that the main peak occurs at 0.7 eV above E_F and therefore can not be used as an electronic channel due to the energy gap of the Si[111]. Also, to control the NDR effect, we have considered doped surfaces, where it is possible to detect the NDR effect for the p-type surface but not for the n-type case. This difference is explained because the number of the channels available, and close to the Fermi level, is lesser for the undoped surface than for the p-type surface. Then the shifting of the states produced by the applied bias diminishes the contribution of the peak that is energetically displaced to the energy gap of the doped surface. In Fig. 13, we can see that the undoped surface and the n-type case do not show important peaks close to the Fermi level in the dI/dV characteristics and the most important contribution comes from the state located 2.3 eV above E_F . If we consider the p-type surface, we can see not only the contribution given by the states related to the dangling bonds of the surface around the Fermi level, but also one peak located at 0.7 eV above E_F and another one at 2.5 eV above E_F .

In summary, the extended Hückel model, used to describe the electronic properties in the system, it is in good agreement when compared with *ab initio* calculations. We have found two stable configurations for the styrene molecule in contact with the surface and both of them can provide interesting properties like the NDR effect. This effect is modulated not only by the electronic molecular levels but also their positions respect to the energy gap of the silicon surface. A semiconductor surface has interesting properties respect to metallic ones, allowing to control transport with the appropriate conditions like doping. In our case, we have a NDR effect of the system at low positive voltage. This effect is also more important when a strong electric field has been considered to shift the molecular states (flat electrode produces a stronger electric field than a sharp tip). The comparison between flat and sharp electrodes has been performed for both configurations finding the same NDR

suppression when a sharp metallic tip is considered. These results strength the idea to use organic molecules as possible components to storage information in electronic devices.

M. E. G. acknowledges the kind hospitality at the IPICYT. This work has been supported by the DFG through the SPP1153. A.H.R. also thanks the support of Conacyt Mexico under the grant J-46247-F. S. E. B. acknowledges the scholarship given by IPICYT and the University of Kassel.

* sbaltaza@ipicyt.edu.mx

- ¹ S. J. Tans, M. H. Devoret, H. Dai, A. Thess, R. E. Smalley, L. J. Geerligs, and C. Dekker, *Nature* **386**, 474 (1997).
- ² R. Sessoli, D. Gatteschi, A. Caneschi, and M. A. Novak, *Nature* **365**, 141 (1993).
- ³ L. Bolotov, N. Uchida, and T. Kanayama, *Eur. Phys. J. D* **16**, 271 (2001).
- ⁴ S. E. Baltazar, M. D. Menech, Saalman, A. H. Romero, and M. E. Garcia, submitted to *J. Appl. Phys.* (2007).
- ⁵ T. Rakshit, G.-C. Liang, A. W. Ghosh, and S. Datta, *Nano Letters* **4**, 1803 (2004).
- ⁶ N. P. Guisinger, M. E. Greene, R. Basu, A. S. Baluch, and M. C. Hersam, *Nano Letters* **4**, 55 (2004).
- ⁷ M. A. Reed, C. Zhou, C. J. Muller, T. P. Burgin, and J. M. Tour, *Science* **278**, 252 (1997).
- ⁸ D. L. Klein, P. L. McEuen, J. E. B. Katari, R. Roth, and A. P. Alivisatos, *Appl. Phys. Lett.* **68**, 2574 (1996).
- ⁹ M. De Menech, U. Saalman, and M. E. Garcia, *Appl. Phys. A* **82**, 113 (2006).
- ¹⁰ M. De Menech, U. Saalman, and M. E. Garcia, *Phys. Rev. B* **73**, 155407 (2006).
- ¹¹ J. Cerda and F. Soria, *Phys. Rev. B* **61**, 7965 (2000).
- ¹² A. R. Williams, P. J. Feibelman, and N. D. Lang, *Phys. Rev. B* **26**, 5433 (1982).
- ¹³ W. Tian, S. Datta, S. Hong, R. Reifenberger, J. I. Henderson, and C. P. Kubiak, *J. Chem. Phys.* **109**, 2874 (1998).
- ¹⁴ Computer code CPMD version 3.9.2, ©*IBM Corp., 1990-2001* and ©*MPI für Festkoerperforschung Stuttgart, 1990-2001*.
- ¹⁵ C. Lee, W. Yang, and R. Parr, *Phys. Rev. B* **37**, 785 (1988).
- ¹⁶ A. D. Becke, *Phys. Rev. A* **38**, 3098 (1988).

- ¹⁷ M. O. Watanabe, T. Miyazaki, and T. Kanayama, Phys. Rev. Lett. **81**, 5362 (1998).
- ¹⁸ A. Khan, Surf. Sci. Rep. **3**, 193 (1983).
- ¹⁹ M. S. Goedecker, J.Hutter, Phys. Rev. B **54**, 1703 (1996).
- ²⁰ M. J. Frisch *et al.*, Computer Code GAUSSIAN 98, *Gaussian, Inc., Pittsburgh, PA, USA* (1998).
<http://www.gaussian.com>
- ²¹ K. C. Pandey and J. C. Phillips, Phys. Rev. B **13**, 750 (1976).
- ²² M. Schlüter, J. R. Chelikowsky, S. G. Louie, and M. L. Cohen, Phys. Rev. B **12**, 4200 (1975).
- ²³ F. G. Allen and G. W. Gobeli, Phys. Rev. **127**, 150 (1962).